Sources and Chemical Characterization of Organic Aerosol during the Summer in the Eastern Mediterranean

Evangelia Kostenidou[1,2], Kalliopi Florou[1,2], Christos Kaltsonoudis[1,2], Maria Tsiflikiotou[1,2], Stergios Vratolis[3], Konstantinos Eleftheriadis[3], and Spyros N. Pandis[1,2,4]

[1]Institute of Chemical Engineering Sciences, ICE-HT, Patras, Greece
[2]Department of Chemical Engineering, University of Patras, Patras, Greece
[3] ERL Institute of Nuclear and Radiological Science & Technology, Energy & Safety, NCRS Demokritos, Attiki, Greece
[4]Department of Chemical Engineering, Carnegie Mellon University, Pittsburgh, USA

Abstract

The concentration and chemical composition of non-refractory fine particulate matter (NR-PM_1) and black carbon (BC) levels were measured during the summer of 2012 in the suburbs of two Greek cities, Patras and Athens, in an effort to better understand the chemical processing of particles in the high photochemical activity environment of the Eastern Mediterranean. The composition of PM_1 was surprisingly similar in both areas demonstrating the importance of regional sources for the corresponding pollution levels. The PM_1 average mass concentration was 9-14 μg m^{-3}. The contribution of sulphate was around 38%, while organic aerosol (OA) contributed approximately 45% in both cases. PM_1 nitrate levels were low (2%). The oxygen to carbon (O:C) atomic ratio was 0.50±0.08 in Patras and 0.47±0.11 in Athens. In both cases PM_1 was acidic.

Positive matrix factorization (PMF) was applied to the high resolution organic aerosol mass spectra obtained by an Aerodyne High Resolution Time-of-Flight Aerosol Mass Spectrometer (HR-ToF-AMS). For Patras five OA sources could be identified: 19%

very oxygenated OA (V-OOA), 38% moderately oxygenated OA (M-OOA), 21% biogenic oxygenated OA (b-OOA), 7% hydrocarbon-like OA (HOA-1) associated with traffic sources and 15% hydrocarbon-like OA (HOA-2) related to other primary emissions (including cooking OA). For Athens the corresponding source contributions were: V-OOA (35%), M-OOA (30%), HOA-1 (18%) and HOA-2 (17%). In both cities the major component was OOA, suggesting that under high photochemical conditions most of the OA in the Eastern Mediterranean is quite aged. The contribution of the primary sources (HOA-1 and HOA-2) was important (22% in Patras and 35% in Athens) but not dominant.

1. Introduction

Atmospheric aerosols can affect human health by causing cardiovascular and respiratory problems (Davidson et al., 2005; Pope and Dockery, 2006), they reduce visibility (Watson, 2002) and influence the energy balance of our planet (IPCC, 2013) by scattering or absorbing radiation and changing cloud reflectivity and lifetime. Submicrometer atmospheric particles mainly consist of sulphates, ammonium, organic matter, nitrates, elemental carbon and metals. Organic aerosol (OA) represents a major fraction of the submicron aerosol mass (Kanakidou et al., 2005; Zhang et al., 2007). The recent development of the Aerodyne HR-ToF-AMS (DeCarlo et al., 2006) allows high time resolution size-resolved measurements of the fine non-refractory inorganic and organic aerosol components. In addition, several techniques have been developed for the deconvolution of the AMS organic mass spectra (Zhang et al., 2011) including custom principal component analysis (Zhang et al., 2005), multiple component analysis (Zhang et al., 2007), and positive matrix factorization (PMF) (Paatero and Tapper 1994; Lanz et al., 2007). The most recent algorithm, the multilinear engine, (ME-2) (Lanz et al., 2008, Canonaco et al., 2013) is a hybrid of chemical mass balance (CMB) and bilinear models (e.g., PMF). The combination of AMS measurements with other instrumentation and the use of the corresponding source apportionment techniques can provide valuable information about the ambient aerosol sources and their chemical characterization. In this study the technique of PMF analysis on HR-ToF-AMS mass spectra is used.

Zhang et al. (2005) showed that summertime OA in a major urban area of the US (Pittsburgh) consisted of oxygenated OA (OOA) and hydrocarbon-like OA (HOA). Lanz et al. (2007) further deconvolved OOA into a more oxygenated OA (OOA-1) and a less oxygenated (OOA-2) component during a summer period in Zurich. They also reported for the fist time a wood burning and a charbroiling factor. Marine OA (MOA) was identified by Crippa et al. (2013a) in Paris during summertime, while Schmale et al. (2013) suggested the existence of an amino-acids/amine OA factor (AA-OA), a methanesulfonic acid OA factor (MSA-OA), a marine oxygenated OA factor (M-OOA) and a sea spray OA factor (SS-OA) on Bird Island in the South Atlantic. The major OA components found usually are OOA and HOA (Ng et al., 2010). In our work the OA sources are investigated, in order to characterize two urban environments in the Eastern Mediterranean.

Most of the studies on air quality in the Eastern Mediterranean and Greece have been based on filter measurements (Manoli et al., 2002; Grivas et al., 2004; Papaefthymiou et al., 2005; Karanasiou et al., 2007; Chrysikou and Samara, 2009) or monitoring PM mass concentrations (Chaloulakou et al., 2003; Vardoulakis and Kassomenos, 2008; Yannopoulos, 2008) in major Greek cities (Athens, Thessaloniki, Patras). During the past years a few field campaigns using continuous PM composition measurement techniques have been conducted in rural/remote areas and urban centres in Greece. At the remote site of Finokalia (Crete) factor analysis on filter samples revealed three sources of coarse particles (crustal, photochemical, and marine aerosols) and two additional factors in the fine mode (residual oil and secondary/combustion aerosols) (Koulouri et al., 2008). For the same site no HOA was detected by PMF analysis of Quadropole AMS data either in the summer or in the winter (Hildebrandt et al., 2010; 2011). For the city of Patras Pikridas et al. (2013) found that the transported pollution accounted for 50% of the $PM_{2.5}$ during the winter and more than 70% during the rest of the year. However, the Eastern Mediterranean urban environment remains not well characterized.

In the Western Mediterranean there have been more measurement campaigns (e.g., Viana et al., 2005; Pérez et al., 2008; Pey et al., 2010; Pandolfi et al., 2014). In Barcelona primary OA accounted for 59% of the OA in the late winter (Mohr et al., 2012). El

Haddad et al. (2013) reported that OOA contributed 80% of the OA mass in Marseille during the summer, while only 5% of the OA was of industrial origin. Nicolas (2013) found that OOA ranged from 70% to 85% of the total OA over a year at the Cape Corsica station. For the same site the oxidation state of the OA during the summer reached extremely high values with f_{44} (the fraction of the AMS *m/z* 44, which is an indicator of the oxidation state) higher than 0.25. Thus the measurements in Western Mediterranean have covered better the different types of environments compared to Eastern Mediterranean.

Despite the previous efforts, there are still several knowledge gaps related to the characterization and OA sources in the Mediterranean Basin. For example the contribution of the primary sources is still uncertain. Fresh OA from diesel exhaust initially resembles HOA but after aging may resemble semi-volatile OOA (SV-OOA) (Jimenez et al., 2009; Chirico et al., 2010). Aged gas phase emissions from diesel engines, scooters and biomass burning may also produce secondary OA (SOA) with mass spectra similar to SV-OOA (Heringa et al., 2012). In addition, volatile organic compounds (VOCs) in chamber experiments form SOA with mass spectra close to SV-OOA (Ng et al., 2010). The conversion of SV-OOA to more oxidized OA is still quite difficult to reproduce in the laboratory. Only recently Platt et al. (2013) showed that after 12 hours of aging of gasoline Euro 5 car emissions, SOA with an O:C ratio of 0.7 was produced resembling LV-OOA. In the field, Hildebrandt et al. (2010) demonstrated that primary emissions are becoming highly oxygenated within 1-2 days of transport under intense photochemical conditions. Recently Bougiatioti et al. (2014) showed that a large fraction of biomass burning OA (BBOA) is transformed to OOA even in the dark in less than a day during the summer in Eastern Mediterranean. The objectives of this work are to:

1) characterize the chemical composition of the PM_1 in two Greek cities in the Eastern Mediterranean using high time resolution instrumentation

2) determine the corresponding OA sources and evaluate the relative significance of the primary versus the oxygenated factors

3) provide insights about the chemical processing of the primary PM

4) compare the mass spectra profiles to the corresponding profiles extracted in previous studies and to

5) assess the overall PM_1 pollution in the Eastern Mediterranean in comparison with other European cities.

2 Experimental

2.1 Measurement campaign

The measurements presented here were part of a larger study, which involved measurements in several areas in Greece (Patras, Athens, Thessaloniki, and Finokalia) both in summer and winter. In this work we will focus on the summer HR-ToF-AMS measurements in Patras and Athens. More information about the summer study is provided in Tsiflikiotou et al. (in preparation).

2.2 Sampling Sites in Patras

Patras has approximately 300,000 inhabitants and is located at the Gulf of Patras, at the foothills of a 2 km high mountain. The major anthropogenic activities include a small industrial zone about 16 km southwest of the city center and a harbor around 2.5 km southwest of the city. The nearest major city is Athens, around 220 km to the east. Measurements in Patras were performed simultaneously at two locations: in the center of the city (38° 14' 46" N, 21° 44' 08" E) and at the Institute of Chemical Engineering Sciences, ICE-HT (38° 17' 52" N, 21° 48' 31" E), which is 8 km (north-east) away from the city center and 1 km (south) from the Patras-Athens highway (Figure S1). The site is surrounded by olive tree fields. A few small settlements are located in a distance of 1 km (southwest and north-east). This paper focuses only on the ICE-HT measurements.

2.3 Instrumentation in Patras

A HR-ToF-AMS from Aerodyne Research Inc. (DeCarlo et al., 2006) was measuring the size-resolved chemical composition of the NR-PM_1 aerosol species. The tungsten filament for electron ionization was run at an accelerating voltage of 70 eV, while the vaporizer temperature was set at 600^{o}C. Alternative runs between V-mode (single stage reflectron) and W-mode (double stage reflectron) were performed with 3 min of measuring time for each mode. In this paper the V-mode data are presented.

A Proton Transfer Reaction Mass Spectrometer (PTR-MS, Ionicon Analytik) was used for the characterization of the volatile organic compounds (VOCs). More details about the VOC measurements are presented in Kaltsonoudis et al. (in preparation). A Scanning Mobility Particle Sizer, (SMPS, classifier model 3080, DMA model 3081, CPC model 3787, TSI) was operated at a sheath flow rate of 5 L min^{-1} and a sample flow rate of 1 L min^{-1}. The SMPS measured the number size distribution in the 10 - 500 nm range. A Multiple-Angle Absorption Photometer (MAAP, Thermo Scientific Inc.) (Petzold and Schönlinner, 2004) was used for the BC measurement. NO_x, SO_2, O_3 and CO concentrations were measured by the corresponding monitors (Teledyne, models T201, 100E, 400E and 300E respectively).

A filter sampler (MetOne SAASS) was used to collect $PM_{2.5}$ samples for inorganic and organic chemical composition analysis. The sampling resolution was 24 h and the flow rate of each filter was 6.7 L min^{-1}. Teflon filters (Whatman 7582 004, 0.2 μm pore size) were used for the measurement of the inorganic anion and cation mass concentrations, using two ion chromatography systems (Metrohm 761 Compact IC). Pre-baked Quartz filters were used for the EC/OC measurement using a laboratory EC/OC analyzer (Sunset Laboratory Inc). More details about the filter extraction procedure are given by Pikridas et al. (2013) and Tsiflikiotou et al. (in preparation).

The HR-ToF-AMS and the PTR-MS measurements covered the period from 8 to 27 of June 2012, while the rest of the instrumentation provided measurements from June 8 to July 26, 2012. All the above mentioned instruments were located at the ICE-HT campus.

2.4 Sampling Site in Athens

Athens is the most densely populated city in Greece with around 4 million inhabitants. The sampling site was at Demokritos National Center for Scientific Research, NCRS (37° 59' 43" N, 23° 48' 57" E), at the municipality of Agia Paraskevi. This is a suburban background site 10 km from the city center located at the foothills of Ymittos mountain and is surrounded by pine trees. This site is close (0.5 km) to the ring highway of Ymittos and approximately 1.5 km away from the Mesogion highway to the north-

184 west. The closest residences are 0.5 km away. The relative position between Patras and
185 Athens sampling site is illustrated in Figure S2.
186
187 **2.5 Instrumentation in the Athens site**
188 For the measurements in Athens we used our mobile laboratory as a fixed station,
189 in which the HR-ToF-AMS, PTR-MS and SMPS (same models as described in session
190 2.3) were placed. An aethalometer (Magee Scientific, AE31) provided the BC
191 concentrations at 880 nm. An SMPS (classifier model 3080 TSI, custom DMA, CPC
192 model 3022, TSI) was operated at a sheath flow rate of 3 L min^{-1} and a sample flow rate
193 of 0.3 L min^{-1} and measured the number size distribution in the 10 - 660 nm range. $PM_{2.5}$
194 was collected on Teflon filters every 24 h for the inorganic composition characterization,
195 while a semi-continuous OC/EC analyzer (Field Instrument, Model 4F, Sunset
196 Laboratory Inc) equipped with a $PM_{2.5}$ inlet and an activated carbon denuder was used for
197 the $PM_{2.5}$ EC/OC measurements with a 3 hr resolution.
198 The sampling period was from 8 to 26 of July 2012. Due to technical problems
199 the HR-ToF-AMS started measuring on the July 12, 2012.
200
201 **2.6 Data Analysis**
202 For HR-ToF-AMS data analysis SQUIRREL v1.51C and PIKA v1.10C (Sueper,
203 2014) with Igor Pro 6.22A (Wavemetrics) were used. For the HR-ToF-AMS organic
204 mass spectra, we used the fragmentation table of Aiken et al. (2009).
205 PMF and ME-2 analysis (Paatero and Tapper, 1994; Lanz et al., 2007; Lanz et al.,
206 2008; Ulbrich et al., 2009; Canonaco et al., 2013) were performed using the HR-ToF-
207 AMS organic mass spectra in order to investigate the different organic aerosol sources.
208 The *m/z's* 12-200 were used as inputs following the procedure of Ulbrich et al. (2009).
209 The Patras HR-ToF-AMS data were corrected for the collection efficiency CE
210 using the algorithm of Kostenidou et al. (2007) with a 2-hour resolution throughout the
211 campaign. A shape factor (χ) of 1 was found to be the most appropriate for this data set
212 (Supplement section 2.A, Figures S3-S4). The average CE was 0.91±0.10 and it was
213 quite higher compared to other studies, which often use a CE of 0.5. One reason could be
214 that the particles entering the HR-ToF-AMS were not dried. Drying the particles usually

decreases the CE because the particles bounce on the vaporizer (Matthew et al., 2008). The R^2 between CE and the ambient relative humidity (RH) was very low (0.02). This low correlation and the high CE values can be explained by the fact that the particles were acidic most of the time (see section 3.1) and probably contained water during all the campaign. Comparing the PM_1 HR-ToF-AMS sulphate (after CE corrections) to the $PM_{2.5}$ filter sulphate measurements a slope of 1.05 and a high correlation (R^2=0.98) were found as shown in Figure S5. This could indicate that most of the $PM_{2.5}$ sulfate was in the submicrometer particles. The average OA density estimated from the above algorithm was 1.34±0.21 g cm^{-3}, which is very close to the organic density calculated for Finokalia during the summer of 2008 (1.35±0.22 g cm^{-3}, Lee et al., 2010).

For Athens the aerosol was not dried before it entered the HR-ToF-AMS, but the particles entering the SMPS were dried to maintain compatibility with long term measurements performed in the site. Thus we modified the algorithm of Kostenidou et al. (2007) converting the ambient HR-ToF-AMS mass distributions to dry mass distributions using the relative humidity (RH) inside the sampling line and calculating the inorganic aerosol water content using the Extended Aerosol Inorganic Model II (E-AIM, Carslaw et al., 1995; Clegg et al., 1998; Massucci et al., 1999). As inputs to the E-AIM model we used the inorganic concentrations of sulphate, ammonium and nitrate and the temperature and RH at the entrance of the HR-ToF-AMS line. The algorithm was run for shape factors 1-1.4 and the optimum solution was selected (i.e. the minimum of the minimum error scores) which corresponded to the optimum CE, organic density, and shape factor (Supplement section 2.B, Figures S6-S7). The average CE was 0.63±0.13. After applying CE corrections the PM_1 HR-ToF-AMS sulphate correlated well with the $PM_{2.5}$ filter sulphate (Figure S8) (R^2=0.91, slope=0.98), once more suggesting that the sulphate in the 1-2.5 μm range was a small fraction of the $PM_{2.5}$ sulfate. The average organic density was 1.15±0.36 g cm^{-3}, lower than in Patras, and the average shape factor was 1.16±0.1 suggesting that a lot of the particles were not spherical.

The angle theta (θ) between the mass spectra vectors was used as a measure of their similarity (Kostenidou et al., 2009). The mass spectra are treated as vectors and the angle θ is calculated by using their internal product. The lower the angle θ is the higher the similarity between the two spectra.

3 Results and Discussion

3.1 Patras

The time series of the mass concentration of the NR-PM_1 components measured by the HR-ToF-AMS and the BC in Patras are shown in Figure 1a. The average PM_1 mass concentration (not including dust) was 8.6 μg m^{-3}. On average, the organic mass concentration was 3.8 μg m^{-3}, sulphate 3.3 μg m^{-3}, ammonium 0.9 μg m^{-3} and BC 0.5 μg m^{-3}. Nitrate was very low around 0.1 μg m^{-3}.

The average OM:OC ratio was 1.80±0.10. The average diurnal profile of O:C is depicted in Figure 2. O:C increased in the early morning hours (2:00-7:00 LT) and during the afternoon (15:00-17:00). The OA average diurnal profile exhibited 3 peaks (Figure S9a), 2 of them (around 8:00-10:00 and 21:00-23:00) were associated with primary sources as the BC increased the same time as well. The OA increase at 11:00-16:00 is related to the formation of secondary species as the solar intensity peaks the same time. The fragments of *m/z* 44 and 57 represented 0.14 and 0.01 of the organic signal correspondingly (Figure S10a).

Combining the OM:OC ratio provided by the high resolution HR-ToF-AMS data and the organic carbon (OC) filter $PM_{2.5}$ measurements we estimated the organic mass (OM) based on the filter samples. Figure S11a shows the correlation between the HR-ToF-AMS and the filters for organics which resulted in an R^2=0.57. This probably implies that the majority of the $PM_{2.5}$ organics were in the PM_1 range.

The PM_1 aerosol as measured by the HR-ToF-AMS was always acidic with an average inorganic cations/anions equivalent ratio of 0.75±0.07. This indicates that there was no available ammonia to fully neutralize the sulphate and thus the formation of PM_1 ammonium nitrate (from ammonia and nitric acid) in the PM_1 was not thermodynamically favorable.

In order to estimate the organic nitrate mass (ONit) contribution to the total nitrate mass (TotNit) we followed the procedure of Farmer et al. (2010):

$$\frac{\mathrm{ONit}}{\mathrm{TotNit}} = \frac{\left(1+\mathrm{R_{ONit}}\right)\times\left(\mathrm{R_{[NO_2^+/NO^+]meas}}-\mathrm{R_{[NO_2^+/NO^+]cal}}\right)}{\left(1+\mathrm{R_{[NO_2^+/NO^+]meas}}\right)\times\left(\mathrm{R_{ONit}}-\mathrm{R_{[NO_2^+/NO^+]cal}}\right)} \quad (1)$$

where $R_{[NO_2^+/NO^+]meas}$ is the measured ratio of NO_2^+/NO^+ ions as a function of time, $R_{[NO_2^+/NO^+]cal}$ is the ratio of NO_2^+/NO^+ ions obtained during NH_4NO_3 calibrations (0.58 on average) and R_{ONit} is a fixed value set to 0.05, as the minimum ratio of NO_2^+/NO^+ observed in this campaign was 0.05. The average organic nitrate fraction was 0.91±0.05, which suggests that most of the nitrate was in the form of organic nitrate (Figure S12a). The correlation between OA and nitrate was moderate (R^2=0.38).

3.2 Athens (Demokritos Station)

On average the PM_1 mass concentration in Athens (not including dust) was 14.2 μg m^{-3}. This is a different period than the one in Patras so direct comparisons could result in erroneous conclusions. A detailed description and intercomparison of the various measurements (including filter samples) performed in Athens and Patras is given in the companion paper by Tsiflikiotou et al. (in preparation). Briefly, these authors found that for the July period the mean concentrations of $PM_{2.5}$ sulphate in Patras and Athens were similar, while $PM_{2.5}$ organics were higher in Patras than in Athens. Figure 1b shows the time series of the concentration of the NR-PM_1 components measured by the HR-ToF-AMS in Athens and the BC measured by the aethalometer. The average organic concentration was 6.6 μg m^{-3}, sulphate 5.3 μg m^{-3}, ammonium 1.4 μg m^{-3} and BC 0.7 μg m^{-3}. Similarly to Patras nitrate levels were low, 0.2 μg m^{-3} on average.

The average O:C mass ratio was 0.47±0.11, lower than in Patras (0.50), because of the higher contribution of primary emissions (Section 3.3.1 and 3.3.2). The average OM:OC ratio was 1.76±0.14. The diurnal cycle of O:C is shown in Figure 2 and is similar to the one in Patras. The O:C exhibited two peaks one in the early morning around 3:00-5:00 LT and a second in the late afternoon 17:00-20:00 LT. The OA profile is characterized by three peaks (Figure S9b). Two of them, around 7:00-12:00 and 20:00-24:00 are related to fresh emissions since the BC follows the same trend. A smaller increase around 14:00-17:00 is probably due to photochemistry. On average f_{44} and f_{57} were 0.13 and 0.02 respectively (Figure S10b).

The OM based on the $PM_{2.5}$ semi-continuous OC/EC measurements was calculated using the OM:OC ratio provided by the HR-ToF-AMS. Figure S11b illustrates

the correlation for the organics between the HR-ToF-AMS and the semi-continuous OC/EC samples. The measurements are in reasonable agreement (R^2=0.48), with the HR-ToF-AMS providing slightly higher concentrations. The scatter observed when comparing the corresponding measurements is due to a number of factors including the positive and negative artifacts of filter measurements, the uncertainties of the corresponding measurements (e.g., due to HR-ToF-AMS CE), and the different size ranges. The negative artifacts of the filter measurements due to evaporation of the collected OA can explain the occurrence of some measurements in which the $PM_{2.5}$ filter-based OA is less than the PM_1 HR-ToF-AMS OA.

The equivalent ratio of PM_1 cations to anions (measured by the HR-ToF-AMS) was on average 0.70±0.09 and thus that the aerosol was acidic. Again free ammonia was not enough to neutralize the sulphate and thus there was no ammonium nitrate observed in the PM_1 fraction.

Applying equation (1) to the Athens data set (with an average $R_{[NO_2^+/NO^+]cal}$=0.68, and R_{ONit} = 0.12), the organic nitrate fraction was 0.89±0.08, indicating that most of the nitrate was actually organic nitrate (Figure S12b). The coefficient of determination between OA and nitrate was R^2=0.62.

3.3 OA sources

3.3.1 Patras

For the PMF analysis both PMF Evaluation Tool, PET, (Lanz et al., 2008; Ulbrich et al., 2009) and ME-2 (Lanz et al., 2008; Canonaco et al., 2013) solutions were examined and evaluated using the HR organic mass spectra. A five factor solution was chosen as the best to describe the major sources of OA in Patras. More information about the choice of the solution is provided in the supplementary information (section 7.A, Figures S13-S21). The factors corresponded to very oxygenated OA (V-OOA, 19%), moderately oxygenated OA (M-OOA, 38%), biogenic oxygenated OA (b-OOA, 21%), HOA-1 (7%) and HOA-2 (15%). The assignment of the factors to specific sources was based on their mass spectra and diurnal profile characteristics: V-OOA had a high contribution of *m/*z 44, M-OOA had a moderate *m/*z 44 contribution, b-OOA was characterized by both biogenic and oxidized OA signatures, HOA-1 was similar to the

literature HOA factor related to traffic emissions and HOA-2 included primary cooking and aged traffic emissions. Overall, the oxygenated OA was the dominant component (78%) and the primary OA accounted for only 22%. The HR mass spectrum of each factor is illustrated in Figure 3a, while their time series are shown in Figure 4a and their average diurnal profiles in Figure 5a.

V-OOA was characterized by a high *m/z* 44 (~22%) with an O:C= 0.81 and is related to aged aerosol (Figure 3a). The V-OOA factor correlated well with sulphate (R^2=0.48) and ammonium (R^2=0.51), which is typical for highly oxygenated OA. Its correlation with nitrate was low (R^2=0.09). The V-OOA diurnal profile was almost flat (Figure 5a). R^2 between V-OOA and individual VOCs measured by the PTR-MS were all less than 0.13.

M-OOA had a pronounced but of lower intensity *m/z* 44 (~16%) and an O:C=0.54 implying aged but less oxidized particles (Figure 3a). Nitrate has been suggested as a tracer for the less oxygenated species (e.g. Lanz et al., 2007; Mohr et al., 2012), however there was very little nitrate during our measurements and most of it was organic nitrate resulting in a weak correlation between the M-OOA and nitrate (R^2=0.04). M-OOA had a very similar pattern with the solar radiation peaking at around 14:00 (local time). M-OOA had low correlation with methyl vinyl ketone (MVK) and methacrolein (MACR) (*m/z* 71, R^2=0.31), hydroxyacetone (*m/z* 75, R^2=0.29), C_5 carbonyls/2-methyl-butene-2-ol (MBO)/methacrylic acid (*m/z* 87, R^2=0.29), terpene oxidation products (*m/z* 113, R^2=0.30) and nopinone (*m/z* 139, R^2=0.28), (Table 1 and Figure S22). Comparing the M-OOA spectrum to the α-pinene SOA spectrum of Heringa et al. (2012) the angle theta was quite high ($\theta=35^o$), while the similarity between the M-OOA and the toluene photo-oxidation SOA spectrum (Kostenidou et al., not published data) was greater ($\theta=16^o$). Thus this factor may include contributions by both anthropogenic and biogenic sources.

The biogenic OOA factor had an f_{44}=0.13 and O:C=0.48 (Figure 3a) which indicates a relatively moderate degree of oxygenation. It was characterized by a distinct *m/z* 82 (mainly composed of $C_5H_6O^+$), an elevated *m/z* 53 (mostly $C_4H_5^+$) and a significant contribution at *m/z* 39 (5%, mainly CH_3O^+). These characteristics were similar to those found at a rural area in Ontario, Canada (Slowik et al., 2011), downtown Atlanta, Georgia, USA (Budisulistiorini et al., 2013), in tropical rainforests in the central Amazon

Basin (Chen et al., 2014) and in Borneo, Malaysia (Robinson et al., 2011) and in Centreville in rural Alabama (Xu et al., 2014) which were associated to secondary OA produced by isoprene photooxidation. Using the HYSPLIT back trajectory model (Draxler and Rolph, 2013), the mass concentration of b-OOA was almost zero when the air masses were coming from the west (e.g. Ionian Sea, 11-15 June, Figure S23), while M-OOA and V-OOA were still high. However, the b-OOA increased in periods (e.g. 10-11 June, 16-17 and 24-26 June) when the air masses passed over the forested mountains of Central Greece (Figure S23), which is an area characterized by high terpene and isoprene emissions (Karl et al., 2009). This supports the biogenic character of this factor. The highest concentration of b-OOA was at 6:00 in the morning on June 16th (5.4 μg m^{-3}). b-OOA exhibited low correlation with isoprene (*m/z* 69, R^2=0.13), isoprene peroxides (*m/z* 101, R^2=0.28) and the first generation isoprene products such as MVK and MACR (*m/z* 71, R^2=0.21) (Table 1). However, it correlated better with acetone (*m/z* 59, R^2=0.35), hydroxyl-acetone (*m/z* 75, R^2=0.41), PAN (*m/z* 77, R^2=0.37), nopinope (*m/z* 139, R^2=0.39) and pinonaldehyde (*m/z* 151, R^2=0.30), Figure S24, which are products of terpenes ozonolysis (Matsunaga et al., 2003; Holzinger et al., 2005; Lee et al., 2006).

HOA-1 was characterized mainly by the *m/z's* 39, 41, 43, 55, 57, 67, 69 and 81 (Figure 3a) which are typical hydrocarbon fragments of fresh traffic emissions (Zhang et al., 2005; Aiken et al., 2009). Its O:C was 0.1 which is in the range found in literature (the HOA factor of Mohr et al. (2012) had an O:C=0.03, while the HOA factor of Ulbrich et al. (2009) had an O:C=0.18). HOA-1 had a medium correlation with BC (R^2=0.38) and nitrate (R^2=0.27). The HOA-1 diurnal profile was characterized by two peaks during the morning (8:00) and evening rush hours (21:00) (Figure 5a). HOA-1 correlated moderately with benzene (*m/z* 79, R^2=0.36), toluene (*m/z* 93, R^2=0.35), xylenes (*m/z* 107, R^2=0.37), C_9 aromatic compounds (*m/z* 121, R^2=0.45). The correlation with NO_x was relatively low (R^2=0.26).

The HOA-2 O:C was 0.21. The HOA-2 spectrums was characterized among others by the *m/z's* 39, 41, 43, 44, 55, 57 and 67 (Figure 3a) which are features of cooking organic aerosol, COA (Ge et al., 2011a, b; Crippa et al., 2013a, b). However, the reported COA spectra (e.g. Ge et al., 2011a, b; Crippa et al., 2013a, b) have lower contributions at *m/z* 44 (0.011-0.022), indicating less oxygenation. The f_{44} in the HOA-2

mass spectrum was 0.034 which implies that this factor may also contain species that have been oxidized to some degree. The HOA-2 diurnal profile had a small peak around 14:00 and a higher one around 22:00, which are consistent with the Greek lunch and dinner periods (Figure 5a). Thus, the HOA-2 in Patras is mainly due to charbroiling of meat cooking OA. The correlation between HOA-2 and BC, nitrate, benzene, toluene, xylenes and C_9 aromatic compounds was moderate (R^2=0.38, 0.38, 0.33, 0.30, 0.33 and 0.43 correspondingly).

During June 16-23 the wind speed was relatively high (average 5.3 m s^{-1}) compared to the rest of the sampling days (average 2.5 m s^{-1}). The contribution of the local sources (HOA-1 and HOA-2) was less than 9% of the OA during that windy period compared to 28% during the remaining days (Figure 4a).

3.3.2 Athens

Four OA factors could be identified in the Athens HR-ToF-AMS data set: V-OOA (35%), M-OOA (30%), HOA-1 (18%) and HOA-2 (17%). A detailed description of the reasons for this selection can be found in the supplement (section 7.B, Figures S25-S33). The corresponding mass spectra are provided in Figure 3b. The time series of the four PMF factors are shown in Figure 4b, while their diurnal cycles in Figure 5b. Similarly to Patras the contribution of the oxygenated OA in Athens was high (65%), while the primary sources contributed 35%.

The very oxidized OA (V-OOA) had an f_{44}=0.18 and O:C=0.68 and showed a good correlation with sulphate (R^2=0.53) and ammonium (R^2=0.50) consistent with the aged character of this factor. The diurnal profile of the V-OOA (Figure 5b) was characterized by a peak around 15:00-18:00, which is probably associated with production of this component in the afternoon over the region. At the same time M-OOA decreased, which indicates that V-OOA is a product of photochemical processing. V-OOA correlated with formic acid (*m/z* 47, R^2=0.47), hexenal (*m/z* 99, R^2=0.42), isoprene peroxides (*m/z* 101, R^2=0.35), terpene oxidation products (*m/z* 113, R^2=0.40), and heptanal (*m/z* 115, R^2=0.42) (Table 1 and Figure S34).

The moderately oxidized OA (M-OOA) was characterized by an f_{44}=0.14 and O:C=0.56 and exhibited a weak correlation with sulphate, ammonium and nitrate

(R^2=0.17, 0.17 and 0.13 respectively). M-OOA increased during the day with a maximum at 12:00-14:00, following the diurnal profile of solar radiation, which implies relatively fast photochemical reactions. M-OOA had a second peak during the night around midnight, which could be an indication of nighttime production or condensation due to the change in temperature between day and night (the average temperature at noon was 32^{o}C, while during the night it decreased to around 21^{o}C). M-OOA did not show any correlation (R^2 less than 0.07) with the measured VOCs.

The HOA-1 O:C was 0.07. Surprisingly it had a rather weak correlation with BC (R^2=0.05) and it also showed a low correlation with nitrate (R^2=0.13). The HOA-1 diurnal profile had 2 peaks, a small increase during the morning (7:00) and a larger peak in the evening hours (20:00), consistent with the contribution of traffic emissions. HOA-1 did not correlate with VOCs characteristic of traffic such as benzene, toluene and xylenes (the R^2 values were correspondingly 0.15, 0.13 and 0.16) and inorganic gases as NO_x (R^2= 0.06). The HOA-1 mass spectrum and time series were very stable for 2 to 5 factorial solutions and for f_{peaks} values from -1 to 1. The R^2 between the HOA-1 of the selected solution and the HOA-1 of the solutions of 2, 3 and 5 factors was always greater than 0.973 (both for the time series and the mass spectra). This weak correlation between the HOA-1 factor and other primary organic pollutants indicates that their concentrations were not dominated by the same sources. For example HOA-1 possibly originated mostly from passenger cars while BC originated from diesel vehicles. The location of the sampling site and the inhomogeneity of the surrounding areas, in combination with the wind direction changes have confounded these effects. The rose plots of HOA-1, BC, NO_x and benzene for wind speeds greater than 1 m s^{-1} indicated that BC, NO_x and benzene had the same origin, while HOA-1 did not. For example at 8:00 LT the HOA-1 was on average coming from southwest (Figure S35-S38) likely from the ring highway of Ymittos, while BC, NO_x and benzene from the north probably influenced by the Mesogion highway.

HOA-2 had an O:C=0.24 and exhibited a good correlation with BC (R^2=0.57). HOA-2 also correlated well with nitrate (R^2=0.75) implying that organic nitrate compounds were possibly emitted or produced along with this OA type. The HOA-2 profile had 2 peaks at around 11:00 and 22:00. The second peak is characteristic of Greek

dinner period, thus part of HOA-2 could be attributed to meat cooking OA. However, the first peak can not be explained by the Greek lunch period. The correlation with the BC implies that HOA-2 and BC had the same origin. Comparing the HOA-2 mass spectrum with aged POA or SOA emissions from other sources such as α-pinene, wood burning, scooter and diesel (Heringa et al., 2012) the angles θ were 19, 19, 28, 17^{o} respectively. This indicates that HOA-2 could include aged diesel emissions since α-pinene is not associated with BC and there were no observed biomass burning events during the sampling period. The HOA-2 factor correlated with the *m/z* 43 (R^2=0.43), acetone (*m/z* 59, R^2=0.44), methyl ethyl ketone (MEK, *m/z* 73, R^2=0.49), benzene (*m/z* 79, R^2=0.62), toluene (*m/z* 93, R^2=0.54), xylenes (*m/z* 107, R^2=0.56), C_9 aromatic compounds (*m/z* 121, R^2=0.58) and C_{10} aromatic compounds (*m/z* 135, R^2=0.55). It also had a good correlation with NO_x (R^2=0.58).

Trying rotations in the f_{peak} range -1 to 1 the correlations between the factors HOA-1 and HOA-2 and traffic markers such as BC and toluene practically did not change. In addition using a fixed HOA spectrum (the HOA mass spectrum of Aiken et al. (2009) and the HOA mass spectrum found in Athens during winter, unpublished results) with *a*=0.1 the correlation between HOA-1 and BC did not improve. All these suggest that our conclusions are robust to the details of the PMF process. Our explanation is that the correlations are affected also by the locations of the various sources around the receptor site and the corresponding wind directions. The fact that these area sources (gasoline cars, diesel cars, cooking activities) did not have a homogeneous spatial distribution can lead to these rather unexpected results.

3.3.3 Comparison of the PMF factors in the two cities

The mass spectra of the V-OOA factors in the two cities were almost the same (θ=6.7^{o}). However, Athens V-OOA exhibited lower f_{44} and O:C ratio (0.18 and 0.68 correspondingly) compared to Patras V-OOA (0.22 and 0.81 respectively). This difference could be partially due to the different periods of the two measurements.

The two M-OOA mass spectra were even more similar to each other (θ=5.4^{o}). A high correlation was also observed between the two HOA-2 mass spectra (θ=5.9^{o}). The Athens HOA-2 was slightly more oxygenated (O:C=0.24), as the oxygenated part of *m/z*

491 43 was more elevated, 65%, compared to 51% observed in Patras HOA-2 and the f_{44} was
492 just slightly higher (0.07), while in Patras HOA-2 was 0.06.
493 The two HOA-1 factors exhibited a lower correlation with each other (θ=22.8^o).
494 The main differences were at *m/z* 41, 43, 55, 57, 69, 71, 81, 83 and 85 which were more
495 abundant in the Athens HOA-1 spectrum, while in the Patras spectrum the f_{44} was higher
496 (0.04) compared to Athens (0.02). In Patras HOA-1 spectrum *m/z* 57 was lower in
497 comparison with *m/z* 55. The O:C in Athens HOA-1 was a little lower (0.07) than in
498 Patras HOA-1 (0.10).
499
500 **3.3.4 Comparing the PMF factors with other studies**
501 Table 2 shows comparisons of the mass spectra of the factors found in the two
502 cities with selected PMF factors from the literature (Aiken et al., 2009; Docherty et al.,
503 2011; Sun et al., 2011; Robinson et al., 2011; Heringa et al., 2012; Mohr et al., 2012, Ge
504 et al., 2012a, b; Crippa et al., 2013a, b; Budisulistiorini et al., 2013; Xu et al., 2014) that
505 have all been extracted using the fragmentation table of Aiken et al. (2009).
506 The two V-OOA factors were quite similar with LV-OOA at Riverside (Docherty
507 et al., 2011), θ=8-10^o, and with LV-OOA at New York City (Sun et al., 2011), θ=11-14^o.
508 They also showed good correlation with LV-OOA measured in Barcelona (Mohr et al.,
509 2012) and Paris (Crippa et al., 2013a, b) θ=13-19^o.
510 M-OOA had moderate to low agreement with the majority of the literature
511 profiles. The lowest angle θ (around 22-24^o) corresponded to the comparison with the
512 SV-OOA found in Mexico City (Aiken et al., 2009). It did however resemble (θ=13-16^o)
513 the toluene SOA spectrum (Kostenidou et al., not published data).
514 The b-OOA factor in Patras correlated moderately with α-pinene SOA, θ=29^o,
515 (Heringa et al., 2012) and the isoprene factor found in Alabama, θ=28^o, (Xu et al.,
516 submitted). However, it had low correlation with the Factor 82, θ=47^o, found in Malaysia
517 (Robinson et al., 2011) and the IEPOX OA factor extracted in Atlanta, θ=76^o,
518 (Budisulistiorini et al., 2013).
519 The HOA-1 factors correlated well with most of the literature HOA profiles,
520 θ=10-25^o.The highest angles (24 and 25^o) corresponded to the comparison with Paris
521 during the winter (Crippa et al., 2013b). The major differences were in the *m/z's* 44 and

28 which were higher than in Paris, *m/z's* 29 and 43 which were lower compared to Paris and *m/z* 39 which was absent in Paris probably due to the unit mass resolution spectra used as input for the Crippa et al. (2013) PMF analysis.

The HOA-2 mass spectra resembled the COA factor extracted in New York City, θ=11-14^{o}, (Sun et al., 2011) and the SOA from diesel VOCs emissions, θ=17^{o}, (Heringa et al., 2012).

Figure S39 summarizes Patras and Athens OA measurements and PMF factors in the Ng triangle (Ng et al., 2010). All the data fall within the triangle.

3.4 Discussion

In both cities the composition of NR-PM_1 was surprisingly similar. Organics' contribution in Patras and Athens was around 45%, which is similar to other areas in Europe: London (UK) 46%, mountain Taunus (Germany) 59%, Melpitz (Germany) 59%, Mace Head (Ireland) 39%, Po Valley (Italy) 33%, and Paris (France) 50% (Cubison et al., 2006; Hings et al., 2007; Poulain et al., 2011; Dall'Osto et al., 2010; Saarikoski et al., 2012; Crippa et al., 2013a). With 38%, sulphate made a larger contribution compared to other studies in Europe during the summer: London 31%, mountain Taunus 24%, Mace Head 32%, Melpitz 22%, Po Valley 9%, and Paris 25% (Cubison et al., 2006; Hings et al., 2007; Dall'Osto et al., 2010; Poulain et al., 2011; Saarikoski et al., 2012; Crippa et al., 2013a). Nitrate contributed very little (less than 2%) and was mostly attributed to organonitrate compounds, in contrast with other European studies where nitrate ranged from 6% (Melpitz) to 39% (Po Valley) (Poulain et al., 2011; Saarikoski et al., 2012) and mainly was ammonium nitrate. The absence of particulate nitrate in PM_1 was also observed at Finokalia (Hildebrandt et al., 2010) and is characteristic of the Eastern Mediterranean. Ammonia levels in this region are quite low (Wichink Kruit et al., 2012) to fully neutralize the existing relatively high sulphate.

The O:C ratios (0.50 for Patras and 0.47 for Athens) were moderately high. The O:C ratio at Finokalia was 0.8 (Hildebrandt et al., 2010), at Cape Corsica 0.9 (Nicolas, 2013), while in Paris 0.38 (Crippa et al., 2013a).

In both cities the OOA was the dominant OA component (78% in Patras and 65% in Athens). This fraction is within the range that has been measured in previous summer

studies in the Mediterranean. For example, the OOA at Finokalia was 100% of the OA (Hildebrandt et al., 2010), in Marseille accounted for 80% (El Haddad et al., 2013), at Cape Corsica 80-85% (Nicolas, 2013), while in Po Valley 61% (Saarikoski et al., 2012).

In Athens 35% of the OA was V-OOA, while in Patras only 19% of the OA was attributed to V-OOA. In addition the V-OOA in Athens was increasing in the afternoon, suggesting its production either locally or regionally. In Patras V-OOA had an almost flat diurnal profile. This difference could be attributed to the different air masses that arrive to each site. According to back trajectory analysis, based on FLEXPART (Stohl et al., 2005) (Figure S40) and HYSPLIT (Draxler and Rolph 2013) during most of the sampling days in Athens the air masses had spent considerable time over the source-poor Aegean Sea, while the majority of the air masses that arrived in Patras were continental and passed over the mountains of Central Greece.

Given the location of the two sites, one would expect to find a marine OA (MOA) factor. The S:C ratio estimated by the AMS is often underestimated in the presence of organosulfates (Farmer et al., 2010; Docherty et al., 2011). To avoid such artifacts we investigated the contribution of MOA applying a constrained solution in the ME-2 using the MOA mass spectrum of Crippa et al. (2013) with a=0.1. For Patras the average MOA concentration for 4, 5, and 6 factors was around 0.04 μg m^{-3} corresponding to 1 percent of the OA mass. For Athens the MOA concentration for the 3, 4 and 5 factor solutions was approximately 0.25 μg m^{-3} (3.7 percent of the OA mass). So if MOA was indeed present its contribution to OA was quite low.

4 Conclusions

During the summer of 2012 the air pollution in Patras (June) and Athens (July) was monitored continuously. The sum of the NR-PM_1 and BC concentration was on average 8.6 μg m^{-3} in Patras and 14.2 μg m^{-3} in Athens. However, the aerosol composition was quite similar in both areas: 45% OA, 38% sulphate, 11% ammonium, 1% nitrate (mostly organic) and 5% BC indicating the importance of regional sources. In both cities the fine aerosol was acidic, which is consistent with the low ammonia levels in the Eastern Mediterranean.

For Patras the average O:C ratio was 0.50±0.08, while in Athens 0.47±0.11. In both cities oxygenated OA was the major component of organic aerosol (78% in Patras and 65% in Athens), indicating the impact of regional pollution in Mediterranean. OOA included a moderately oxygenated OA and a very oxygenated OA component. In Patras a biogenic oxidized OA factor could be identified, which was related to air masses passing over the forests of Central Greece. A primary OA factor (HOA-2) was found in both cities attributed to primary emissions such as meat cooking. This factor may also contain oxygenated primary emissions (e.g., aged diesel emissions). Hydrocarbon-like OA mainly from traffic emissions was also indentified, accounting only for 7-18% of the OA and indicating that new emission control technologies applied to vehicles during the last decade have reduced dramatically the levels of the corresponding primary OA.

Acknowledgments. The authors are grateful to Evangelos Louvaris and Magda Psichoudaki for their assistance with the measurements in Patras. This research was supported by the European Research Council Project ATMOPACS (Atmospheric Organic Particulate Matter, Air Quality and Climate Change Studies) (Grant Agreement 267099) and the European FP7 project PEGASOS. This research has been co-financed by the European Union (European Social Fund – ESF) and Greek national funds through the Operational Program "Education and Lifelong Learning" of the National Strategic Reference Framework (NSRF) - Research Funding Program: THALES.

References

Aiken, A. C., Salcedo, D., Cubison, M. J., Huffman, J. A., DeCarlo, P. F., Ulbrich, I. M., Docherty, K. S., Sueper, D., Kimmel, J. R., Worsnop, D. R., Trimborn, A., Northway, M., Stone, E. A., Schauer, J. J., Volkamer, R. M., Fortner, E., de Foy, B., Wang, J., Laskin, A., Shutthanandan, V., Zheng, J., Zhang, R., Gaffney, J., Marley, N. A., Paredes-Miranda, G., Arnott, W. P., Molina, L. T., Sosa, G., and Jimenez, J. L.: Mexico City aerosol analysis during MILAGRO using high resolution aerosol mass spectrometry at the urban supersite (T0) – Part 1: Fine particle composition and organic source apportionment, Atmos. Chem. Phys., 9, 6633-6653, 2009.

614 Bougiatioti, A., Stavroulas, I., Kostenidou, E., Zarmpas, P., Theodosi, C., Kouvarakis, G.,
615 Canonaco, F., Prévôt, A. S. H., Nenes, A., Pandis, S. N., and Mihalopoulos, N.:
616 Processing of biomass-burning aerosol in the eastern Mediterranean during summertime,
617 Atmos. Chem. Phys., 14, 4793-4807, 2014.
618
619 Budisulistiorini, S. H., Canagaratna, M. R., Croteau, P. L., Marth, W. J., Baumann, K.,
620 Edgerton, E. S., Shaw, S. L., Knipping, E. M., Worsnop, D. R., Jayne, J. T., Gold, A., and
621 Surratt, J. D.: Real-time continuous characterization of secondary organic aerosol derived
622 from isoprene epoxydiols in downtown Atlanta, Georgia, using the Aerodyne Aerosol
623 Chemical Speciation Monitor, Environ. Sci. Technol., 47, 5686–5694, doi:
624 10.1021/es400023n, 2013.
625
626 Canonaco, F., Crippa, M., Slowik, J. G., Baltensperger, U., and Prévôt, A. S. H.: SoFi, an
627 IGOR-based interface for the efficient use of the generalized multilinear engine (ME-2)
628 for the source apportionment: ME-2 application to aerosol mass spectrometer data,
629 Atmos. Meas. Tech., 6, 3649-3661, 2013.
630
631 Carslaw, K. S., Clegg, S. L., and Brimblecombe, P.: A thermodynamic model of the
632 system HCl-HNO_3-H_2SO_4-H_2O, including solubilities of HBr, from <200K to 328 K, J.
633 Phys. Chem., 99, 11557–11574, 1995.
634
635 Chaloulakou A., Kassomenos, P., Spyrellis, N., Demokritou, P., and Koutrakis, P.:
636 Measurements of PM_{10} and $PM_{2.5}$ particle concentrations in Athens, Greece, Atmos.
637 Environ., 37, 649–660, 2003.
638
639 Chen, Q., Farmer, D. K., Rizzo, L. V., Pauliquevis, T., Kuwata, M., Karl, T. G.,
640 Guenther, A., Allan, J. D., Coe, H., Andreae, M. O., Pöschl, U., Jimenez, J. L., Artaxo, P.,
641 and Martin, S. T.: Fine-mode organic mass concentrations and sources in the Amazonian
642 wet season (AMAZE-08), Atmos. Chem. Phys. Discuss., 14, 16151-16186, 2014.
643

644 Chirico, R., DeCarlo, P. F., Heringa, M. F., Tritscher, T., Richter, R., Prévôt, A. S. H.,
645 Dommen, J., Weingartner, E., Wehrle, G., Gysel, M., Laborde, M., and Baltensperger,
646 U.: Impact of aftertreatment devices on primary emissions and secondary organic aerosol
647 formation potential from in-use diesel vehicles: results from smog chamber experiments,
648 Atmos. Chem. Phys., 10, 11545–11563, 2010.
649
650 Chrysikou L.P. and Samara C.: Seasonal variation of the size distribution of urban
651 particulate matter and associated organic pollutants in the ambient air, Atmos. Environ.,
652 43, 4557- 4569, 2009.
653
654 Clegg, S., Brimblecombe, L., P. and Wexler, A. S.: A thermodynamic model of the
655 system H^+-NH_4^+-SO_4^{2-}-NO_3^--H_2O at tropospheric temperatures. J. Phys. Chem. A102,
656 2137–2154, doi: 10.1021/jp973043j, 1998.
657
658 Crippa M., El Haddad I., Slowik J., G., DeCarlo P. F., Mohr, C., Heringa, M., F, Chirico,
659 R., Marchand, N., Sciare, J., Urs, B., and Prévôt, A. S. H.: Identification of marine and
660 continental aerosol sources in Paris using high resolution aerosol mass spectrometry, J.
661 Geophys. Res, doi: 118, 1950-1963, doi: 10.1002/jgrd.50151, 2013a.
662
663 Crippa, M., DeCarlo, P. F., Slowik, J. G., Mohr, C., Heringa, M. F., Chirico, R., Poulain,
664 L., Freutel, F., Sciare, J., Cozic, J., Di Marco, C. F., Elsasser, M., Jose, N., Marchand,
665 N., Abidi, E., Wiedensohler, A., Drewnick, F., Schneider, J., Borrmann, S., Nemitz, E.,
666 Zimmermann, R., Jaffrezo, J.-L., Prévôt, A. S. H., and Baltensperger, U.: Wintertime
667 aerosol chemical composition and source apportionment of the organic fraction in the
668 metropolitan area of Paris, Atmos. Chem. Phys., 13, 961–981, 2013b.
669
670 Cubison, M. J., Alfarra, M. R., Allan, J., Bower, K. N., Coe, H., McFiggans, G. B.,
671 Whitehead, J. D., Williams, P. I., Zhang, Q., Jimenez, J. L., Hopkins, J., and Lee, J.: The
672 characterization of pollution aerosol in a changing photochemical environment, Atmos.
673 Chem. Phys., 6, 5573-5588, 2006.
674

675 Dall'Osto, M., Ceburnis, D., Martucci, G., Bialek, J., Dupuy, R., Jennings, S. G.,
676 Berresheim, H., Wenger, J., Healy, R., Facchini, M. C., Rinaldi, M., Giulianelli, L.,
677 Finessi, E., Worsnop, D., Ehn, M., Mikkilä, J., Kulmala, M., and O'Dowd, C. D.: Aerosol
678 properties associated with air masses arriving into the North East Atlantic during the
679 2008 Mace Head EUCAARI intensive observing period: an overview, Atmos. Chem.
680 Phys., 10, 8413-8435, 2010.
681
682 Davidson, C. I., Phalen, R. F., and Solomon, P. A.: Airborne particulate matter and
683 human health: A review, Aerosol Sci. Tech., 39, 737–749, 2005.
684
685 DeCarlo, P.F., Kimmel, J. R., Trimborn, A., Northway, M. J., Jayne, J. T., Aiken, A. C.,
686 Gonin, M., Fuhrer, K., Horvath, T., Docherty, K., Worsnop, D. R., and Jimenez, J. L.:
687 Field-Deployable, High-Resolution, Time-of-Flight Aerosol Mass Spectrometer,
688 Analytical Chemistry, 78, 8281-8289, 2006.
689
690 Docherty, K. S., Aiken, A. C., Huffman, J. A., Ulbrich, I. M., DeCarlo, P. F., Sueper, D.,
691 Worsnop, D. R., Snyder, D. C., Peltier, R. E., Weber, R. J., Grover, B. D., Eatough, D. J.,
692 Williams, B. J., Goldstein, A. H., Ziemann, P. J., and Jimenez, J. L.: The 2005 Study of
693 Organic Aerosols at Riverside (SOAR-1): Instrumental intercomparisons and fine particle
694 composition, Atmos. Chem. Phys., 11, 12387-12420, 2011.
695
696 Draxler, R. R., and Rolph, G. D., 2013. HYSPLIT (HYbrid Single-Particle Lagrangian
697 Integrated Trajectory) Model access via NOAA ARL READY Website
698 (http://ready.arl.noaa.gov/HYSPLIT.php). NOAA Air Resources Laboratory, Silver
699 Spring, MD.
700
701 El Haddad, I., D'Anna, B., Temime-Roussel, B., Nicolas, M., Boreave, A., Favez, O.,
702 Voisin, D., Sciare, J., George, C., Jaffrezo, J.-L., Wortham, H., and Marchand, N.:
703 Towards a better understanding of the origins, chemical composition and aging of
704 oxygenated organic aerosols: case study of a Mediterranean industrialized environment,
705 Marseille, Atmos. Chem. Phys., 13, 7875-7894, 2013.

706 Farmer, D.K., Matsunaga, A., Docherty, K. S., Surratt, J. D., Seinfeld, J. H., Ziemann P.
707 J., and Jimenez, J. L., Response of an aerosol mass spectrometer to organonitrates and
708 organosulfates and implications for atmospheric chemistry. Proceedings of the National
709 Academy of Sciences, 107, 6670-6675, doi: 10.1073/pnas.0912340107, 2010.

710 Ge, X., Setyan, A., Sun, Y., and Zhang, Q.: Primary and secondary organic aerosols in
711 Fresno, California during wintertime: Results from high resolution aerosol mass
712 spectrometry, J. Geophys. Res., 117, D19301, 10.1029/2012JD018026, 2012a.

713 Ge, X., Zhang, Q., Sun, Y., Ruehl, C. R., and Setyan, A.: Effect of aqueous-phase
714 processing on aerosol chemistry and size distribution in Fresno, California, during
715 wintertime, Environ. Chem., 9, 221-235, 10.1071/EN11168, 2012b.

716 Grivas, G., Chaloulakou, A, Samara, C., and Spyrellis, N.: Spatial and temporal variation
717 of PM_{10} mass concentrations within the greater area of Athens, Greece, Water, Air and
718 Soil Pollution, 158, 357-371, 2004.
719
720 Heringa, M. F., DeCarlo, P. F., Chirico, R., Tritscher, T., Clairotte, M., Mohr, C.,
721 Crippa, M., Slowik, J. G., Pfaffenberger, L., Dommen, J., Weingartner, E.,
722 Prévôt, A. S. H., and Baltensperger, U.: A new method to discriminate secondary organic
723 aerosols from different sources using high-resolution aerosol mass spectra, Atmos. Chem.
724 Phys., 12, 2189-2203, 2012.
725
726 Hildebrandt, L., Engelhart, G. J., Mohr, C., Kostenidou, E., Lanz, V. A., Bougiatioti, A.,
727 DeCarlo, P. F., Prévôt, A. S. H., Baltensperger, U., Mihalopoulos, N., Donahue, N. M.,
728 and Pandis, S. N.: Aged organic aerosol in the Eastern Mediterranean: the Finokalia
729 Aerosol Measurement Experiment – 2008, Atmos. Chem. Phys., 10, 4167–4186, 2010.
730
731 Hildebrandt, L., Kostenidou, E., Lanz, V. A., Prévôt, A. S. H., Baltensperger, U.,
732 Mihalopoulos, N., Laaksonen, A., Donahue, N. M., and Pandis, S. N.: Sources and
733 atmospheric processing of organic aerosol in the Mediterranean: insights from aerosol
734 mass spectrometer factor Analysis, Atmos. Chem. Phys., 11, 12499–12515, 2011.

Hings S.S., Walter, S., Schneider, J., Borrmann, S., and Drewnick, F.: Comparison of a Quadrupole and a Time-of-Flight Aerosol Mass Spectrometer during the Feldberg Aerosol Characterization Experiment 2004, Aerosol Science and Technology, 41, 679 - 691, 2007.

Holzinger, R., Lee, A., Paw, K. T., and Goldstein, U. A. H.: Observations of oxidation products above a forest imply biogenic emissions of very reactive compounds, Atmos. Chem. Phys., 5, 67-75, doi: 10.5194/acp-5-67-2005, 2005.

IPCC: Climate Change 2013 – The Physical Science Basis, Contribution of Working Group I to the Fourth Assessment Report of the IPCC, Cambridge University Press, Cambridge, 2013.

Jimenez, J. L., Canagaratna, M. R., Donahue, N. M., Prévôt, A. S. H., Zhang, Q., Kroll, J. H., DeCarlo, P. F., Allan, J. D., Coe, H., Ng, N. L., Aiken, A. C., Docherty, K. S., Ulbrich, I. M., Grieshop, A. P., Robinson, A. L., Duplissy, J., Smith, J. D., Wilson, K. R., Lanz, V. A., Hueglin, C., Sun, Y. L., Tian, J., Laaksonen, A., Raatikainen, T., Rautiainen, J., Vaattovaara, P., Ehn, M., Kulmala, M., Tomlinson, J. M., Collins, D. R., Cubison, M. J., Dunlea, E. J., Huffman, J. A., Onasch, T. B., Alfarra, M. R., Williams, P. I., Bower, K., Kondo, Y., Schneider, J., Drewnick, F., Borrmann, S., Weimer, S., Demerjian, K., Salcedo, D., Cottrell, L., Griffin, R., Takami, A., Miyoshi, T., Hatakeyama, S., Shimono, A., Sun, J. Y., Zhang, Y. M., Dzepina, K., Kimmel, J. R., Sueper, D., Jayne, J. T., Herndon, S. C., Trimborn, A. M., Williams, L. R., Wood, E. C., Middlebrook, A. M., Kolb, C. E., Baltensperger, U., and Worsnop, D. R.: Evolution of organic aerosols in the atmosphere, Science, 326, 1525–1529, 2009.

Holzinger, R., Lee, A., Paw, K. T., and Goldstein, U. A. H.: Observations of oxidation products above a forest imply biogenic emissions of very reactive compounds, Atmos. Chem. Phys., 5, 67-75, 2005.

766 Kanakidou, M., Seinfeld, J. H., Pandis, S. N., Barnes, I., Dentener, F. J., Facchini, M. C.,
767 Van Dingenen, R., Ervens, B., Nenes, A., Nielsen, C. J., Swietlicki, E., Putaud, J. P.,
768 Balkanski, Y., Fuzzi, S., Horth, J., Moortgat, G. K., Winterhalter, R., Myhre, C. E. L.,
769 Tsigaridis, K., Vignati, E., Stephanou, E. G., and Wilson, J.: Organic aerosol and global
770 climate modeling: a review, Atmos. Chem. Phys., 5, 1053–1123, 2005.
771
772 Kaltsonoudis, C., Kostenidou, E., Florou, K., Psichoudaki, M., and Pandis, S. N.:
773 Temporal variability of VOCs in the Eastern Mediterranean (in preparation).
774
775 Karanasiou, A. A., Sitaras, I. E., Siskos, P. A., and Eleftheriadis, K.: Size distribution and
776 sources of trace metals and n-alkanes in the Athens urban aerosol during summer, Atmos.
777 Environ., 41, 2368–2381, 2007.
778
779 Karl, M., Guenther, A., Köble, R., Leip, A., and Seufert, G.: A new European plant-
780 specific emission inventory of biogenic volatile organic compounds for use in
781 atmospheric transport models, Biogeosciences, 6, 1059-1087, 2009.
782
783 Kostenidou, E., Pathak, R. K., and Pandis, S. N.: An algorithm for the calculation of
784 secondary organic aerosol density combining AMS and SMPS data, Aerosol Sci.
785 Technol., 41, 1002–1010, 2007.
786
787 Kostenidou, E., Lee, B. H., Engelhart, G. J., Pierce, J. R., and Pandis, S. N.: Mass spectra
788 deconvolution of low, medium and high volatility biogenic secondary organic aerosol,
789 Environ. Sci. Technol., 43, 4884–4889, 2009.
790
791 Koulouri, E., Saarikoski, S., Theodosi, C., Markaki, Z., Gerasopoulos, E., Kouvarakis, G.,
792 Makela, T., Hillamo, R., and Mihalopoulos, N.: Chemical composition and sources of
793 fine and coarse aerosol particles in the Eastern Mediterranean, Atmos. Environ., 42,
794 6542–6550, 2008.
795

796 Lanz, V. A., Alfarra, M. R., Baltensperger, U., Buchmann, B., Hueglin, C., and Prévôt, A.
797 S. H.: Source apportionment of submicron organic aerosols at an urban site by factor
798 analytical modeling of aerosol mass spectra, Atmos. Chem. Phys., 7, 1503–1522, 2007.

799 Lanz, V. A., Alfarra, M. R., Baltensperger, U., Buchmann, B., Hueglin, C., Szidat, S.,
800 Wehrli, M. N., Wacker, L., Weimer, S., Caseiro, A., Puxbaum, J., and Prévôt, A. S. H.:
801 Source attribution of submicron organic aerosols during wintertime inversions by
802 advanced factor analysis of aerosol mass spectra, Environ. Sci. Technol., 42, 214-220,
803 2008.

804 Lee, A., Goldstein, A. H., Keywood, M. D., Gao, S.,Varutbangkul, V., Bahreini, R., Ng,
805 N. L., Flagan, R. C., and Seinfeld, J. H.: Gas-phase products and secondary aerosol yields
806 from the ozonolysis of ten different terpenes, J. Geophys. Res., 111, D07302, doi:
807 10.1029/2005JD006437, 2006.

808 Lee, B. H., Kostenidou, E., Hildebrandt, L., Riipinen, I., Engelhart, G. J., Mohr, C.,
809 DeCarlo, P. F., Mihalopoulos, N., Prévôt, A. S. H., Baltensperger, U. and Pandis S. N.:
810 Measurement of the ambient organic aerosol volatility distribution: application during the
811 Finokalia Aerosol Measurement Experiment (FAME-2008), Atmos. Chem. Phys., 10,
812 12149–12160, 2010.

813 Manoli E., Voutsa D. and Samara C.: Chemical characterization and source
814 identification/apportionment of fine and coarse air particles in Thessaloniki, Greece,
815 Atmos. Environ., 36, 949-961, 2002.
816
817 Massucci, M., Clegg, S. L., and Brimblecombe, P.: Equilibrium partial pressures,
818 thermodynamic properties of aqueous and solid phases, and Cl_2 production from aqueous
819 HCl and HNO_3 and their mixtures, J. Phys. Chem. A 103, 4209 4226, doi:
820 10.1021/jp9847179, 1999.

821 Matsunaga, S., Mochida, M., and Kawamura, K.: Growth of organic aerosols by biogenic
822 semi-volatile carbonyls in the forest atmosphere, Atmos. Environ., 37, 2045–2050, 2003.

823 Matthew, B. M., Middlebrook, A. M., and Onasch, T. B.: Collection efficiencies in an
824 Aerodyne Aerosol Mass Spectrometer as a function of particle phase for laboratory
825 generated aerosols, Aerosol Sci. Technol., 42, 884–898, 2008.

826 Mohr, C., DeCarlo, P. F., Heringa, M. F., Chirico, R., Slowik, J. G., Richter, R., Reche,
827 C., Alastuey, A., Querol, X., Seco, R., Peñuelas, J., Jimenez, J. L., Crippa, M.,
828 Zimmermann, R., Baltensperger, U., and Prévôt, A. S. H.: Identification and
829 quantification of organic aerosol from cooking and other sources in Barcelona using
830 aerosol mass spectrometer data, Atmos. Chem. Phys., 12, 1649–1665, 2012.
831
832 Nicolas, J. : Caractérisation physico-chimique de l'aérosol troposphérique en
833 Méditerranée : Sources et Devenir, Ph.D. thesis, Université de Versailles Saint-Quentin-
834 en-Yvelines, Ecole Doctorale des Sciences de l'Environnement d'Ile-de-France, Paris,
835 France, 2013.
836
837 Ng, N.L., Canagaratna, M. R., Zhang, Q., Jimenez, J. L., Tian, J., Ulbrich, I. M., Kroll, J.
838 H., Docherty, K. S., Chhabra, P. S., Bahreini, R., Murphy, S. M., Seinfeld, J. H.,
839 Hildebrandt, L., Donahue, N. M., DeCarlo, P. F., Lanz, V. A., Prévôt, A. S. H., Dinar, E.,
840 Rudich, Y., and Worsnop D. R.: Organic aerosol components observed in northern
841 hemispheric datasets measured with Aerosol Mass Spectrometry. Atmos. Chem. Phys, 10,
842 4625-4641, 2010.
843
844 Paatero, P. and Tapper, U.: Positive matrix factorization – a nonnegative factor model
845 with optimal utilization of error-estimates of data values, Environmetrics, 5, 111–126,
846 1994.
847
848 Pandolfi, M., Querol, X., Alastuey, A., Jimenez, J. L., Jorba, O., Day, D., Ortega, A.,
849 Cubison, M. J., Comerón, A., Sicard, M., Mohr, C., Prévôt, A. S. H., Minguillón, M. C.,
850 Pey, J., Baldasano, J. M., Burkhart, J. F., Seco, R., Peñuelas, J., van Drooge, B. L.,
851 Artiñano, B., Di Marco, C., Nemitz, E., Schallhart, S., Metzger, A., Hansel, A., Llorente,
852 J., Ng, S., Jayne, J., and Szidat, S.: Effects of sources and meteorology on particulate

853 matter in the Western Mediterranean Basin: An overview of the DAURE campaign, J.
854 Geophys. Res. Atmos., 119, 4978–5010, doi: 10.1002/2013JD021079, 2014.
855
856 Papaefthymiou, H., Kritidis, P., Anousis, J., and Sarafidou, J.: Comparative assessment of
857 natural radioactivity in fallout samples from Patras and Megalopolis, Greece, J. of
858 Environomental Radioactivity, 78, 249-265, 2005.
859
860 Pérez, N., Pey, J., Castillo, S., Viana, M., Alastuey, A., and Querol, X.: Interpretation of
861 the variability of levels of regional background aerosols in the Western Mediterranean,
862 Science of the Total Environment, 407, 527-540, 2008.
863
864 Petzold, A., and Schönlinner, M: Multi-angle absorption photometry – a new method for
865 the measurement of aerosol light absorption and atmospheric black carbon, J. Aerosol
866 Sci., 35, 421-441, 2004.
867
868 Pey, J., Pérez, N., Querol, X., Alastuey, A., Cusack, M., and Reche, C.: Intense winter
869 atmospheric pollution episodes affecting the Western Mediterranean, Science of the Total
870 Environment, 408, 1951-1959, 2010.

871 Pikridas, M., Tasoglou, A., Florou, K., and Pandis, S. N.: Characterization of the origin
872 of fine particulate matter in a medium size urban area in the Mediterranean, Atmos.
873 Environ., 80, 264–274, 2013.
874
875 Platt, S. M., El Haddad, I., Zardini, A. A., Clairotte, M., Astorga, C., Wolf, R.,
876 Slowik, J. G., Temime-Roussel, B., Marchand, N., Ježek, I., Drinovec, L., Močnik, G.,
877 Möhler, O., Richter, R., Barmet, P., Bianchi, F., Baltensperger, U., and Prévôt, A. S. H.:
878 Secondary organic aerosol formation from gasoline vehicle emissions in a new mobile
879 environmental reaction chamber, Atmos. Chem. Phys., 13, 9141-9158, 2013.
880
881 Pope, C. A. and Dockery, D. W.: Health effects of fine particulate air pollution: Lines
882 that connect, J. Air Waste Manage., 56, 709–742, 2006.

Poulain, L., Spindler, G., Birmili, W., Plass-Dülmer, C., Wiedensohler, A., and Herrmann, H.: Seasonal and diurnal variations of particulate nitrate and organic matter at the IfT research station Melpitz, Atmos. Chem. Phys., 11, 12579-12599, 2011.

Robinson, N. H., Hamilton, J. F., Allan, J. D., Langford, B., Oram, D. E., Chen, Q., Docherty, K., Farmer, D. K., Jimenez, J. L., Ward, M. W., Hewitt, C. N., Barley, M. H., Jenkin, M. E., Rickard, A. R., Martin, S. T., McFiggans, G., and Coe, H.: Evidence for a significant proportion of secondary organic aerosol from isoprene above a maritime tropical forest, Atmos. Chem. Phys., 11, 1039–1050, 2011.

Saarikoski, S., Carbone, S., Decesari, S., Giulianelli, L., Angelini, F., Canagaratna, M., Ng, N. L., Trimborn, A., Facchini, M. C., Fuzzi, S., Hillamo, R., and Worsnop, D.: Chemical characterization of springtime submicrometer aerosol in Po Valley, Italy, Atmos. Chem. Phys., 12, 8401-8421, 2012.

Schmale, J., Schneider, J., Nemitz, E., Tang, Y. S., Dragosits, U., Blackall, T. D., Trathan, P. N., Phillips, G. J., Sutton, M., and Braban C. F.: Sub-Antarctic marine aerosol: significant contributions from biogenic sources, Atmos. Chem. Phys., 13, 8669–8694, 2013.

Slowik, J. G., Brook, J., Chang, R. Y.-W., Evans, G. J., Hayden, K., Jeong, C.-H., Li, S.-M., Liggio, J., Liu, P. S. K., McGuire, M., Mihele, C., Sjostedt, S., Vlasenko, A., and Abbatt, J. P. D.: Photochemical processing of organic aerosol at nearby continental sites: contrast between urban plumes and regional aerosol, Atmos. Chem. Phys., 11, 2991–3006, 2011.

Stohl, A., Forster, V., Frank, A., Seibert, P., & Wotawa, G.: Technical Note: The Lagrangian particle dispersion model FLEXPART version 6.2, Atmos. Chem. Phys., 5, 2461–2474, 2005.

914 Sueper, D.: ToF-AMS High Resolution Analysis Software – Pika, online available at:
915 http://cires.colorado.edu/jimenez-group/ ToFAMSResources/ToFSoftware, last access: 1
916 December 2014.
917
918 Sun, Y. L., Zhang, Q., Schwab, J. J., Demerjian, K. L., Chen, W. N., Bae, M. S., Hung, H.
919 M., Hogrefe, O., Frank, B., Rattigan, O. V., and Lin, Y. C.: Characterization of the
920 sources and processes of organic and inorganic aerosols in New York city with a high-
921 resolution time-of-flight aerosol mass spectrometer, Atmos. Chem. Phys., 11, 1581–1602,
922 2011.
923
924 Tsiflikiotou, T., Papanastasiou, D., Zarmpas, P., Paraskevopoulou, D., Diapouli, E.,
925 Kostenidou, E., Kaltsonoudis, C., Bougiatioti, A., Theodosi, C., Kouvarakis, G.,
926 Liakakou, E., Vassilatou, V., Siakavaras, D., Biskos, G., Eleftheriadis, K., Gerasopoulos,
927 E., Mihalopoulos, N., and Pandis, S. N.: Spatial distribution of summertime particulate
928 matter and its composition in Greece (in preparation).
929
930 Ulbrich, I. M., Canagaratna, M. R., Zhang, Q., Worsnop, D. R., and Jimenez, J. L.:
931 Interpretation of organic components from Positive Matrix Factorization of aerosol mass
932 spectrometric data, Atmos. Chem. Phys., 9, 2891–2918, 2009.
933
934 Vardoulakis S. and Kassomenos P.: Sources and factors affecting PM10 levels in two
935 European cities: Implications for local air quality management, Atmos. Environ., 4142,
936 3949-3963, 2008.
937
938 Viana, M., Pérez, C., Querol, X., Alastuey, A., Nickovic, S., and Baldasano J. M.: Spatial
939 and temporal variability of PM levels and composition in a complex summer atmospheric
940 scenario in Barcelona (NE Spain), Atmos. Environ., 39, 5343-5361, 2005.
941
942 Watson, J. G.: Visibility: Science and regulation, J. Air Waste Manage., 52, 628–713,
943 2002.
944

945 Wichink Kruit, R. J., Schaap, M., Sauter, F. J., van Zanten, M. C., and van Paul, W. A.
946 J.: Modeling the distribution of ammonia across Europe including bi-directional surface-
947 atmosphere exchange, Biosciences, 9, 5261–5277, 2012.
948
949 Yannopoulos, P.C.: Long-term assessment of airborne particulate concentrations in Patras,
950 Greece, Fresenius Environ. Bull., 17, 608-616, 2008.
951
952 Xu, L., Guo, H., Boyd, C. M., Klein, M., Bougiatioti, A., Cerully, K, M., Hite, J. R.,
953 Isaacman-VanWertz, G., Kreisberg, N. M., Knote, C., Olson, K., Koss, A., Goldstein, A.
954 H., Hering, S. V., de Gouw, J., Baumann, K., Lee, S-H., Nenes, A., Weber, R. J., Ng, N.
955 L.: Effects of anthropogenic emissions on aerosol formation from isoprene and
956 monoterpenes in the Southeastern United States, P. Natl. Acad. Sci., 112, 37-42, doi:
957 10.1073/pnas.1417609112, 2014.
958
959 Zhang, Q., Alfarra, M. R., Wornsop, D. R., Allan, J. D., Coe, H., Canagaratna, M., and
960 Jimenez, J. L.: Deconvolution and quantification of hydrocarbon-like and oxygenated
961 organic aerosols based on aerosol mass spectrometry, Environ. Sci. Technol., 39, 4938-
962 4952, 2005.

963 Zhang, Q., Jimenez, J. L., Canagaratna, M. R., Allan, J. D., Coe, H., Ulbrich, I., Alfarra,
964 M. R., Takami, A., Middlebrook, A. M., Sun, Y. L., Dzepina, K., Dunlea, E., Docherty,
965 K., De- Carlo, P. F., Salcedo, D., Onasch, T., Jayne, J. T., Miyoshi, T., Shimono, A.,
966 Hatakeyama, S., Takegawa, N., Kondo, Y., Schneider, J., Drewnick, F., Borrmann, S.,
967 Weimer, S., Demerjian, K., Williams, P., Bower, K., Bahreini, R., Cottrell, L., Griffin, R.
968 J., Rautiainen, J., Sun, J. Y., Zhang, Y. M., and Worsnop, D. R.: Ubiquity and dominance
969 of oxygenated species in organic aerosols in anthropogenically-influenced Northern
970 Hemisphere midlatitudes, Geophys. Res. Lett., 34, L13801, doi: 10.1029/2007gl029979,
971 2007.

972

973 Zhang, Q., Jimenez, J., Canagaratna, M., Ulbrich, I., Ng, N., Worsnop, D., and Sun, Y.:
974 Understanding atmospheric organic aerosols via factor analysis of aerosol mass
975 spectrometry: a review, Anal. Bioanal.Chem., 401, 3045-3067, 2011.
976
977
978
979
980
981
982
983
984
985
986
987
988

989

990 **Table 1**. Correlations of the M-OOA and b-OOA factors (Patras) and the V-OOA factor

991 (Athens) with various VOCs measured by the PTR-MS.

R^2	Patras M-OOA	Patras b-OOA	Athens V-OOA
m/z 43	0.29	0.13	0.39
m/z 47 (formic acid)	0.21	0.09	0.47
m/z 59 (acetone, glyoxal)	0.21	0.35	0.32
m/z 71 (MVK, MACR)	0.31	0.21	0.20
m/z 73 (MEK)	0.24	0.25	0.29
m/z 75 (hydroxyacetone)	0.29	0.41	0.30
m/z 77 (PAN)	0.16	0.37	0.16
m/z 81 (terpenes)	0.19	0.26	0.12
m/z 87 (MBO, C5, methacrylic acid)	0.29	0.31	0.38
m/z 95 (2 vinyl furan, phenol)	0.17	0.31	0.36
m/z 99 (hexenal)	0.19	0.30	0.42
m/z 101 (isoprene hyperoxides,hexanal)	0.17	0.28	0.35
m/z 103 (MPAN)	0.23	0.28	
m/z 113 (chlorobenzene, terpenes $+O_3$)*	0.30	0.37	0.40
m/z 115 (heptanal)	0.16	0.32	0.42
m/z 137 (monoterpenes)	0.20	0.24	0.1
m/z 139 (nopinone)	0.28	0.39	0.19
m/z 151 (pinonaldehyde)	0.17	0.30	0.17

992

993

994

995

996

997

998

999

1000

1001
1002 **Table 2**. Correlations between PMF factors from Patras and Athens and PMF factors
1003 from selected studies.

	Angle (degrees) with V-OOA Patras	**Angle (degrees) with V-OOA Athens**
LV-OOA Mexico City[1]	21	20
LV-OOA Riverside[2]	10	8
LV-OOA Barcelona[3]	18	16
LV-OOA Paris (SIRTA) summer[4]	19	15
OOA Paris (SIRTA), winter[5]	13	15
LV-OOA New York City[6]	14	11
LV-OOA Fresno[7,8]	36	30

1004

	Angle (degrees) with M-OOA Patras	**Angle (degrees) with M-OOA Athens**
SV-OOA Mexico City[1]	24	22
SV-OOA Riverside[2]	42	39
SV-OOA Barcelona[3]	33	31
SV-OOA Paris (SIRTA) summer[4]	42	39
SV-OOA New York City[6]	30	27
α-pinene ozonolysis SOA aged[9]	35	32
Toluene photooxidation (HONO) SOA[10]	16	13

1005

	Angle (degrees) with HOA-1 Patras	**Angle (degrees) with HOA-1 Athens**
HOA Mexico City[1]	13	14
HOA Riverside[2]	20	10
HOA Barcelona[3]	22	11
HOA Paris (SIRTA) summer[4]	16	18
HOA Paris (SIRTA), winter[5]	25	24
HOA New York City[6]	12	10
HOA Fresno[7,8]	11	11

1006

	Angle (degrees) with HOA-2 Patras	**Angle (degrees) with HOA-2 Athens**
COA Barcelona[3]	77	77
COA Paris (SIRTA), summer[4]	30	34
COA Paris (SIRTA), winter[5]	30	28
COA Paris (LHVP), winter[5]	27	31
COA New York City[6]	11	14
COA Fresno[7,8]	28	33
Aged VOCs diesel emissions[9]	17	17
α-pinene ozonolysis SOA aged[9]	20	19
Toluene photooxidation (HONO) SOA[10]	26	23

1007
1008
1009
1010

	Angle (degrees) with b-OOA Patras
α-pinene ozonolysis SOA aged[9]	29
Factor 82[11]	47
IEPOX OA[12]	76
Isoprene-OA[13]	28

[1]Aiken et al. (2009), [2]Docherty et al. (2011), [3]Mohr et al. (2012), [4]Crippa et al. (2013a), [5]Crippa et al. (2013b), [6]Sun et al. (2011), [7,8]Ge et al. (2012a,b), [9]Heringa et al. (2012), [10]Kostenidou et al., (not published data),[11]Robinson et al. (2011), [13]Budisulistiorini et al. (2013), [13]Xu et al., (2014),

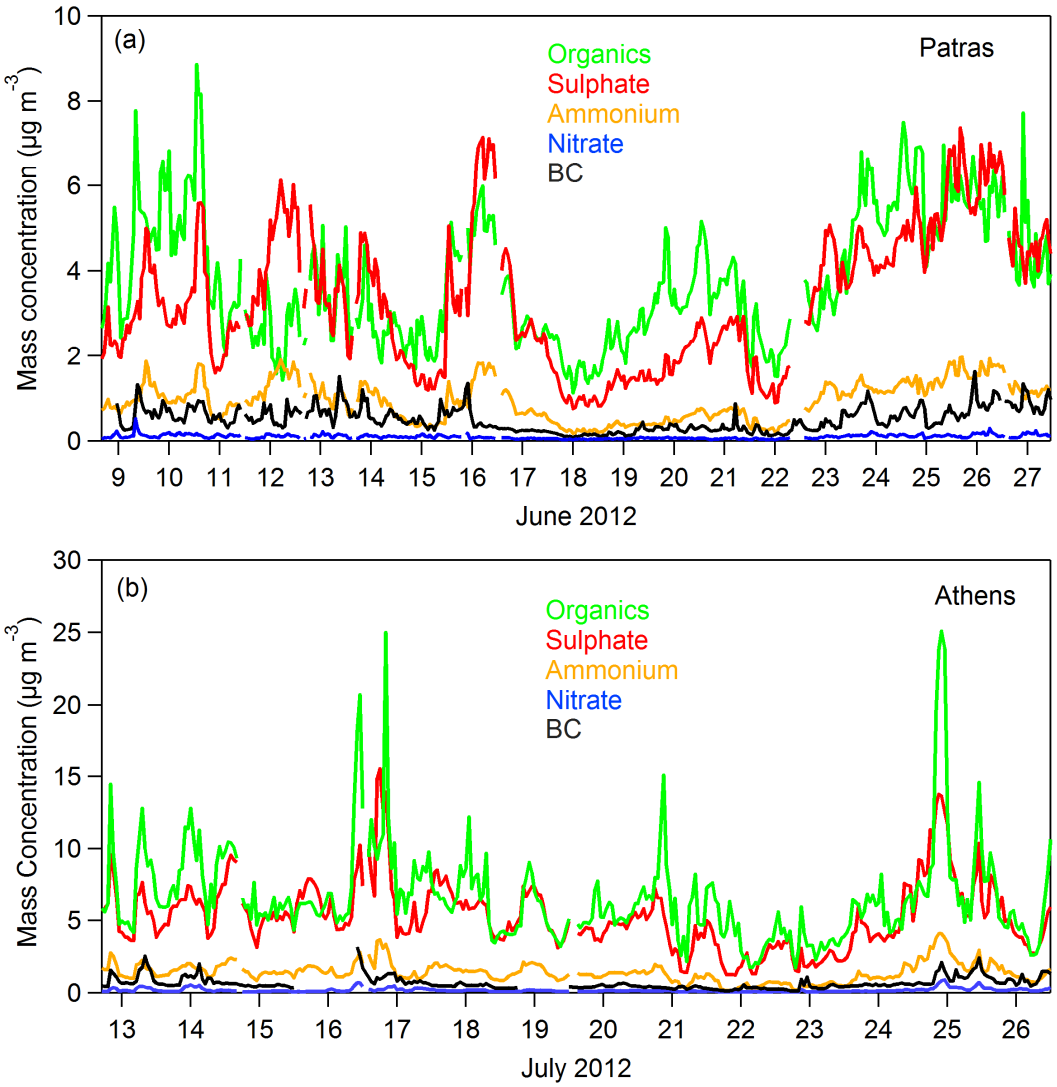

Figure 1. Time series of organics, sulphate, ammonium and nitrate mass concentration measured by the HR-ToF-AMS (corrected for the CE) and BC a) for Patras and b) for Athens. The BC was provided by MAAP for Patras measurements and by an aethalometer for Athens.

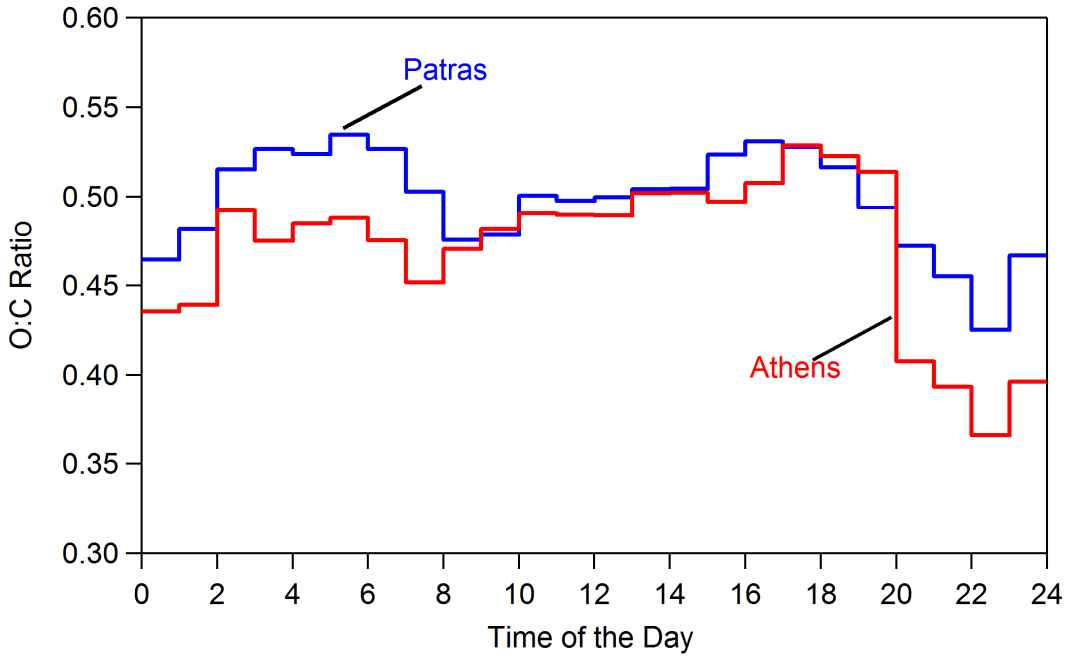

Figure 2. Diurnal profile of O:C ratio for Patras (blue line) and Athens (red line) data set. The O:C was calculated with the Aiken et al. (2009) fragmentation table.

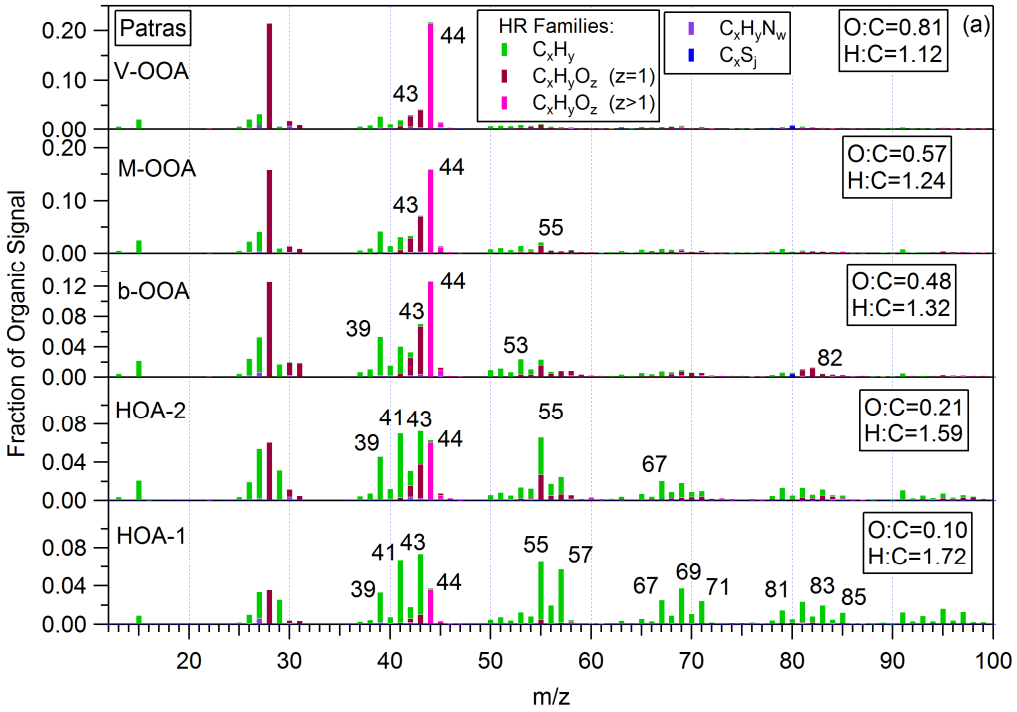

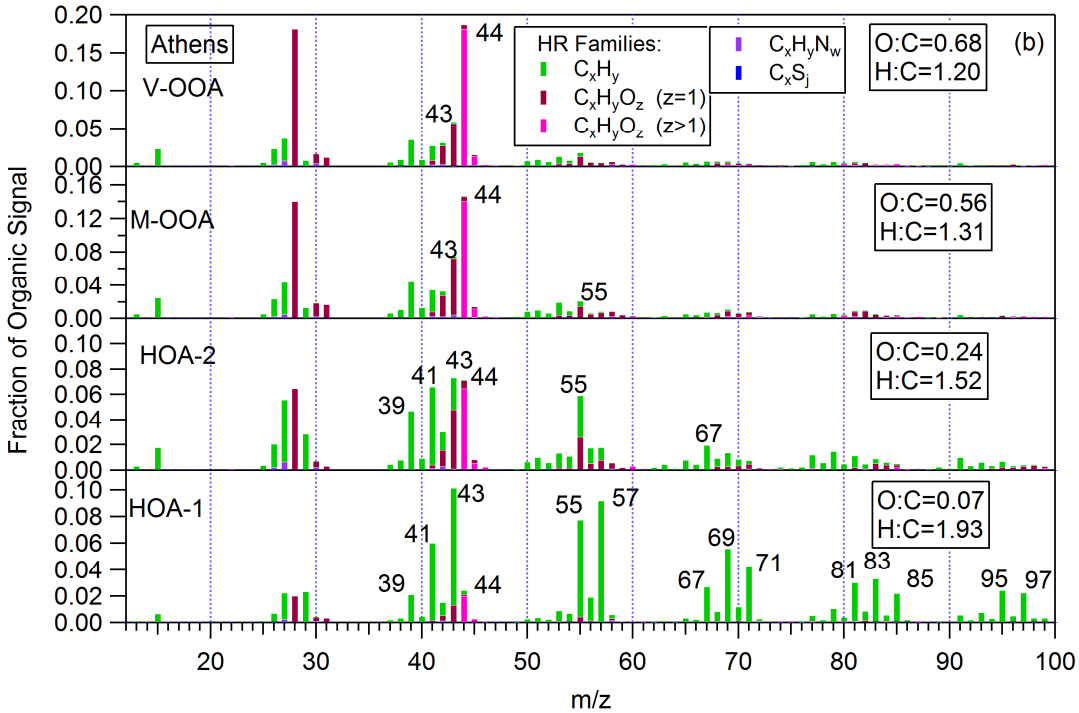

Figure 3. HR mass spectra profiles of the sources found a) in Patras and b) in Athens.

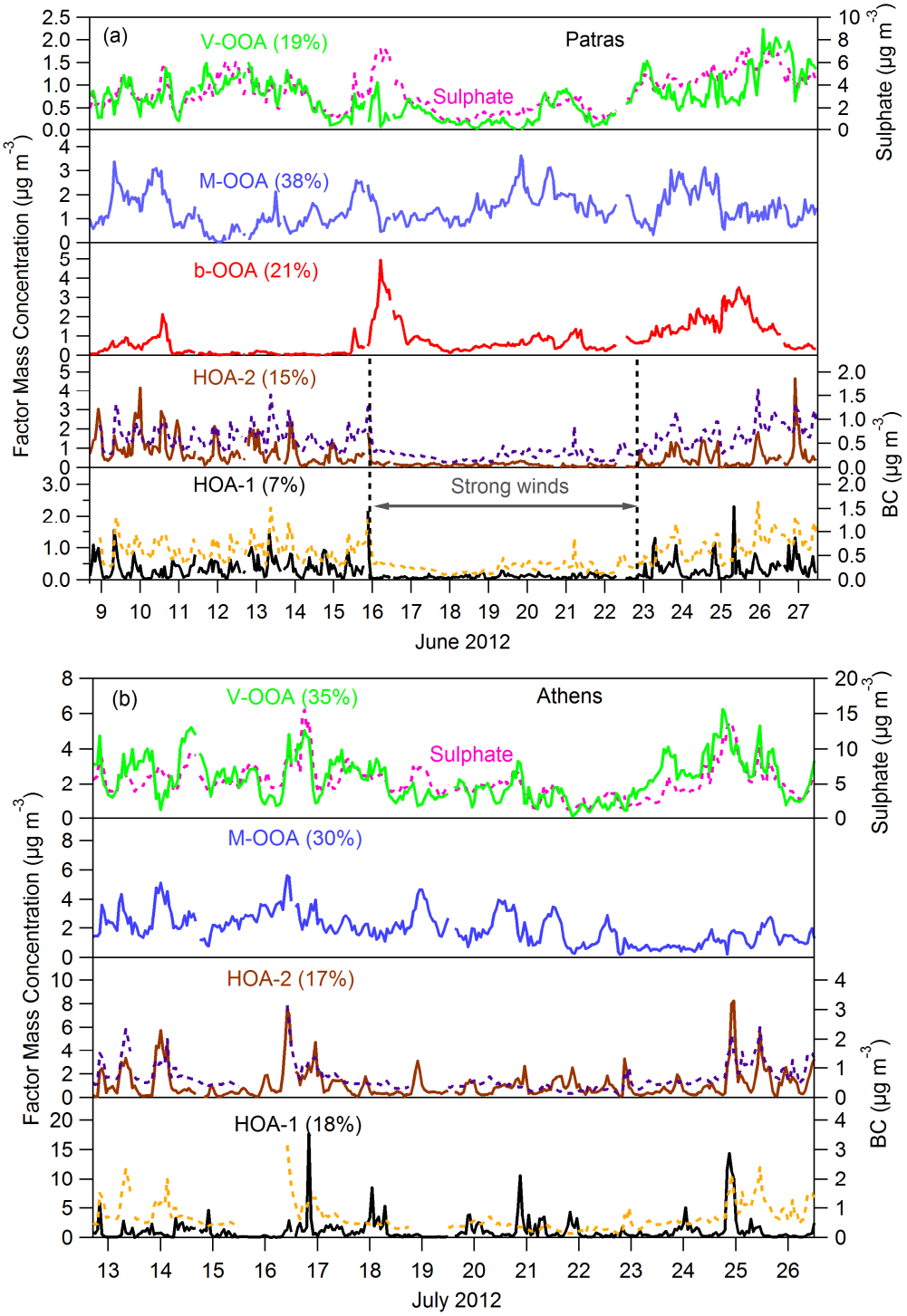

Figure 4. Time series a) of the five PMF factors using HR organic mass spectra for Patras and b) of the four PMF factors found in Athens. For the Patras measurements the HOA-1 and HOA-2 contribution was very low between the 16th and 23rd of June 2012 due to the high wind speed during that period.

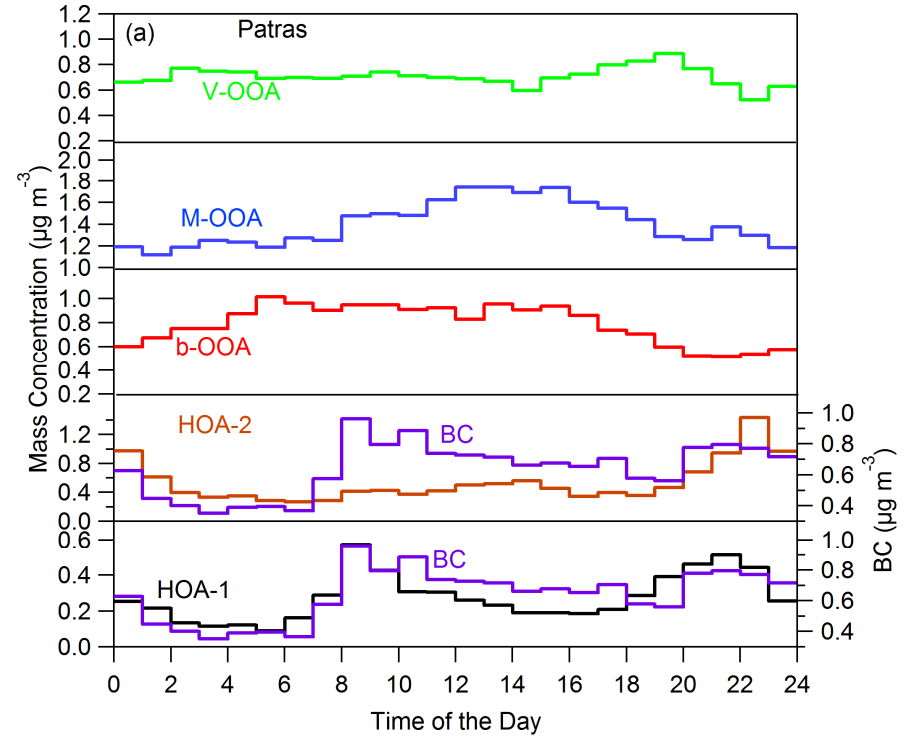

1102

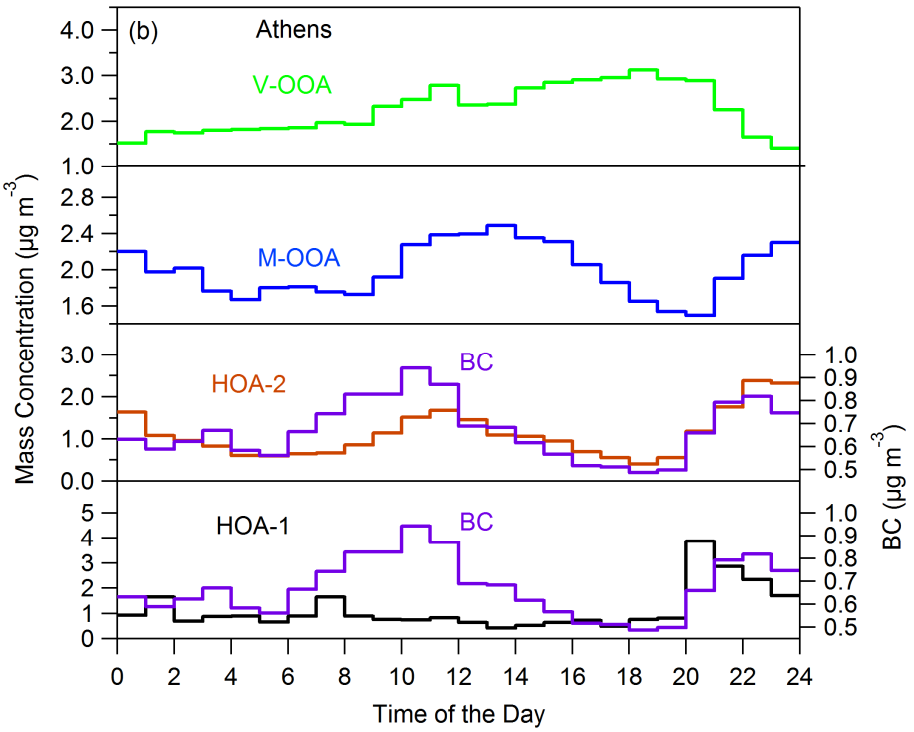

1103
1104

1105 **Figure 5**. Diurnal cycles of the PMF factors a) in Patras and b) in Athens.

1106